Nanotechnology **24** (2013) 465401 (5pp) doi:10.1088/0957-4484/24/46/465401

Effects of ion concentration on thermally-chargeable double-layer supercapacitors

Hyuck Lim[1], Weiyi Lu[2], Xi Chen[3] and Yu Qiao[1,2]

[1] Program of Materials Science and Engineering, University of California—San Diego, La Jolla, CA 92093, USA
[2] Department of Structural Engineering, University of California—San Diego, La Jolla, CA 92093-0085, USA
[3] Department of Earth and Environmental Engineering, Columbia University, New York, NY 10027, USA

E-mail: yqiao@ucsd.edu

Received 3 February 2012, in final form 2 October 2012
Published 22 October 2013
Online at stacks.iop.org/Nano/24/465401

Abstract
The concept of thermally-chargeable supercapacitor was discussed and validated experimentally. As two double-layer supercapacitor-type devices were placed at different temperatures and connected, due to the thermal dependence of surface charge structures, the electrode potentials became different, and thermal energy could be harvested and stored as electric energy. The important effect of ion concentration was investigated. The results were quite different from the prediction of conventional surface theory, which should be attributed to the unique behaviors of the ions confined in the nanoporous electrodes.

(Some figures may appear in colour only in the online journal)

1. Introduction

As harvesting, storage, and utilization of thermal energy has been an active research topic for centuries (e.g. [1, 2]), low-grade heat (LGH), thermal energy associated with low-temperature heat sources with temperature (T) lower than 250 °C, has attracted increasing attention (e.g. [3]). In such a low temperature range, many technologies that work well at higher temperatures become economically and/or energetically inefficient. For instance, most of direct heat storage methods based on phase transformation or chemical reactions are irrelevant for LGH [4]. A few available LGH storage materials, e.g. paraffin [5], are too expensive for large-scale industrial systems.

An intrinsic difficulty comes from the low thermal energy density of LGH. One possible solution is to harvest, convert, and store LGH in other forms, e.g. electric energy, so that systems of higher energy densities can be employed. Converting LGH to electric energy also helps transport and directly utilize the harvested and stored energy.

However, conventional thermal-to-electric energy conversion (TEEC) techniques work poorly in the temperature range of LGH. A TEEC system typically works in between a high-temperature heat source and a low-temperature heat sink. Its energetic efficiency can be calculated as $\zeta = \zeta_c \zeta_s$, where $\zeta_c = \Delta T/T_h$ is the Carnot cycle limit and ζ_s is the system efficiency, with $\Delta T = T_h - T_l$ and T_h and T_l the temperatures of the heat source and the heat sink, respectively. As ΔT of LGH is small, the Carnot cycle limit becomes low and, thus, ζ_s must be ultrahigh to achieve an acceptable overall efficiency. Indirect TEEC techniques, such as organic Rankin cycle (ORC) machines and turbine engines, do not meet this requirement. They are often used for applications where $\Delta T > 350$ °C [6], e.g. in coal power plants and in concentrated solar thermal energy farms. They demand bulky, massive, and expensive components such as heat exchangers and pumps. The numerous moving parts increase the installation, operational, and maintenance costs. Direct TEEC technology is often achieved by using thermoelectric materials, which, again, due to the low value of ζ_s in the LGH range, cannot be widely applied in engineering practice.

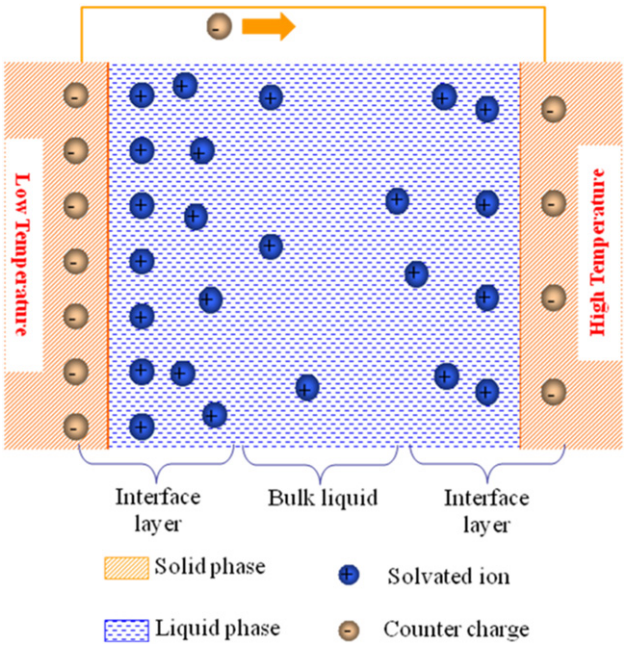

Figure 1. Schematics of the thermally induced capacitive effect. As the temperatures of the two identical solid surfaces are different, the effective surface ion densities become different. Thus, when the two solid surfaces are connected, a net output potential difference can be generated between them.

Note that the Seebeck effect, the working mechanism of thermoelectric materials, is not the only phenomenon that is both thermally and electrically related. Many other phenomena, e.g. the thermally induced capacitive effect to be discussed in this paper (figure 1), also involve energy conversion between heat and electricity. While in the past they were regarded as trivial, with the development of novel materials and energy techniques, these concepts should be re-investigated.

Consider two identical supercapacitor-type devices, as depicted in figure 2(a). Each cell is a half-supercapacitor, consisting of a nanoporous electrode immersed in an electrolyte solution. Figure 2(b) shows a double-layer (DL) supercapacitor. As a voltage is applied across the anode and the cathode, ions would be adsorbed at the electrode surfaces, and electric energy is stored as surface charges. Usually, the electrodes are nanoporous, so that the specific surface areas, A, are ultrahigh ($\sim 10^3$ m^2 g^{-1} of electrode). The large value of A greatly amplifies the system capacitance. Depending on the liquid and electrode materials, the working voltage ranges from a fraction of to a few volts [7].

As described in figure 1, a high-ion-density surface layer can be formed spontaneously at an electrode–liquid interface, even without an external voltage [8–10]. The excess surface ions induce surface charges in the electrode phase, leading to the formation of electrode potential (ϕ). The electrode potential is thermally dependent: When temperature varies, as the mobility of surface ions is changed, the surface ion density becomes different, so does ϕ. Therefore, the two electrodes in figures 1 and 2(a) are of different potentials. When they are connected, charges would move from the high-potential end to the low-potential end, converting the absorbed thermal energy

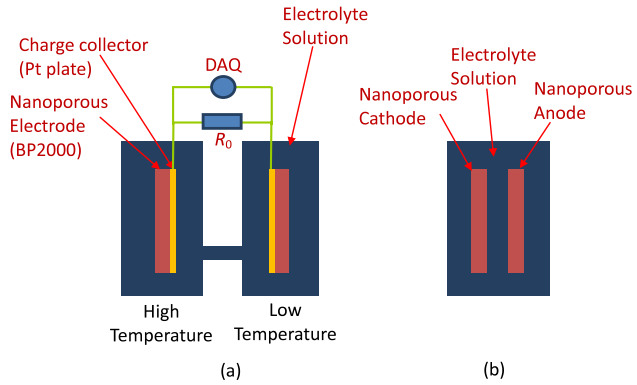

Figure 2. Schematics of (a) a thermally-chargeable supercapacitor (TCS) and (b) a double-layer (DL) supercapacitor.

to electric energy. This capacitive process is fundamentally different from the Seebeck effect, as the charge motion and the thermal conduction are separated. Hence, thermal shorting, which causes the low energetic efficiency of thermoelectric materials, can be prevented. Due to the presence of the liquid phase, such a system may not work at a high temperature, but may have a high performance in the LGH range, as the thermal sensitivity of electrode potential can be much higher than the Seebeck coefficients of thermoelectric materials. Such capacitive effect based systems will be referred to as thermally-chargeable supercapacitors (TCS) in the following discussion.

2. Experimental details

To validate the feasibility of TCS for LGH, we investigated a nanoporous carbon (Cabot BP2000). The as-received material was in powder form. By using a Micromeritics ASAP2000 Analyzer, a gas absorption analysis was performed and the range of nanopore size distribution was determined as 2–100 nm, with the modal value at 3 nm. The specific surface area was about 1200 m^2 g^{-1}. It was refluxed in acetone for 4 h, and then dried in vacuum at 80 °C for 10 h. In a stainless steel mold, the refluxed carbon powders were compressed at 400 MPa for 5 min, so as to form electrode disks. The mass of each disk was nearly 100 mg. In each electrode disk, no binders were employed.

Two identical nanoporous carbon (NC) disks were firmly pressed on platinum (Pt) sheets and soaked in electrolyte solution in two separate polypropylene (PP) cells, as depicted in figure 2(a). The surface area of the Pt sheet was about 100 mm^2. They were used as charge collectors. The liquid volume in each cell was 50 ml. The liquid is an aqueous solution of lithium chloride (LiCl), with the ion concentration in the range of 0.1 M to 3.7 M.

One cell was kept at room temperature by a cold water bath (21 °C), and the temperature of the other cell was raised by a Corning PC-220 Hot Plate, with a constant rate of 3 °C min^{-1}. The temperature was monitored continuously by type-K thermocouples. The liquid phase in the two cells was connected by a salt bridge, which was 5 mm in diameter and 30 mm long. The open-circuit voltage between the two

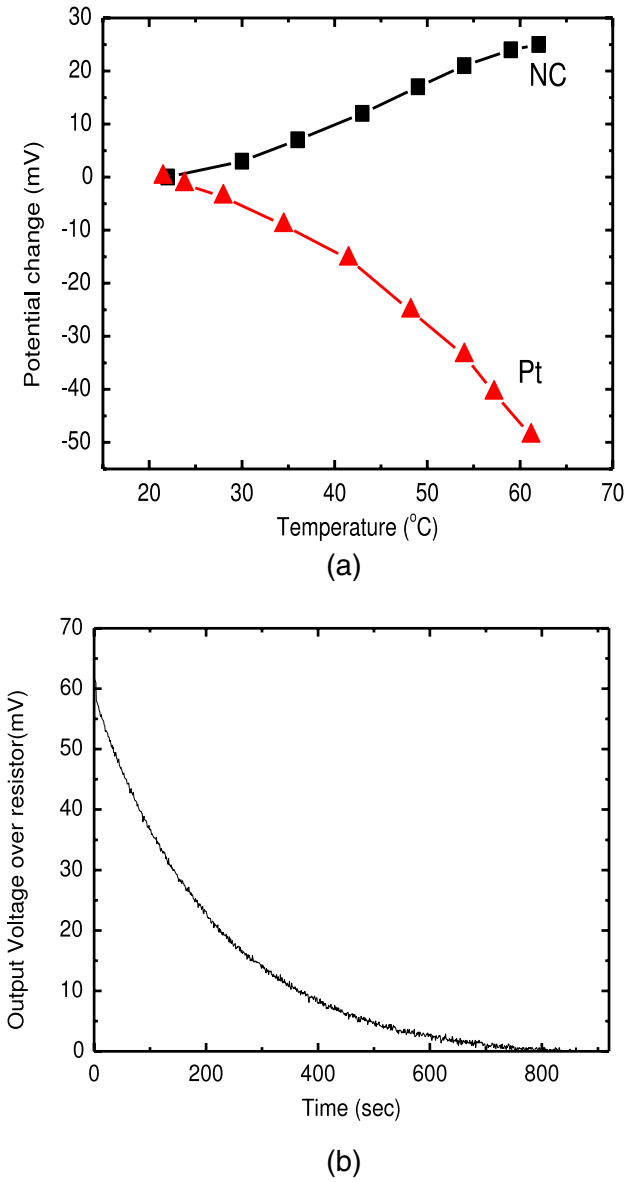

Figure 3. (a) Typical voltage–temperature curves of the nanoporous carbon (NC) and the charge collector (Pt), with the ion concentration, C, being 1 M. (b) A typical discharge curve for the NC based system.

charge collectors, V, was measured by a National Instrument SCB68 data acquisition (DAQ) system. Figure 3(a) shows a typical V–ΔT curve. The temperature sensitivity of V, $\mathrm{d}V/\mathrm{d}T$, is shown in figure 4. When the high-temperature cell reached about 60 °C, the two charge collectors were connected through an external resistor, $R_0 = 250\ \Omega$. A typical discharge curve is shown in figure 3(b). Reference experiments were performed by using a similar setup with the NC disks being removed; that is, only the Pt charge collectors were tested.

3. Results and discussion

From the data of the NC based system in figure 3, it can be seen that as ΔT increases, the amplitude of the output

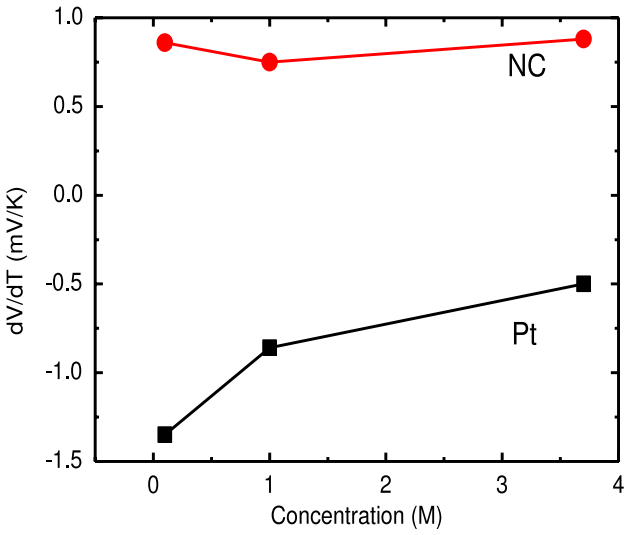

Figure 4. The temperature sensitivity of NC and Pt ($\mathrm{d}V/\mathrm{d}T$) as a function of the ion concentration.

voltage, $|V|$ rises monotonically. The value of $|V|$ reflects the electrode potential difference between the two electrodes, having contributions from both the NC disks and the Pt charge collectors. However, because the surface area of the Pt sheet is much smaller than that of the NC disk by a few orders of magnitude, its effective capacitance is negligible. As the Pt–liquid interface and the NC–liquid interface are in parallel, the output voltage should be governed by the NC phase. The magnitude of $\mathrm{d}V/\mathrm{d}T$ of such as a TCS is around 0.8 mV °C^{-1}, much higher than the Seebeck coefficients of thermoelectric materials. When ΔT is only around 50 °C, the output voltage can be a few tens of mV.

During discharging, because the temperature does not vary, no thermal-to-electric energy conversion would take place. When the new equilibrium is reached, the output voltage vanishes as the electric energy is dissipated by R_0. The electric energy comes from the stored energy in the NC electrodes, harvested from LGH. The total energy can be calculated as $\int (V^2/R_0)\,\mathrm{d}t$, with t denoting the discharging time. The testing data indicate that the energy density of the NC is more than 0.1 J g^{-1}, which corresponds to a specific capacitance around 55 F g^{-1}, much higher than that of ordinary thermoelectric materials [8]. The specific output power was nearly 2.3 mW g^{-1}.

Without the nanoporous phase, the reference system demonstrates quite regular characteristics. As ΔT increases, $\mathrm{d}V/\mathrm{d}T$ is negative; that is, the electrode potential decreases, as it should, since at a higher temperature the solvated ions in the interface double layer are more mobile and the effective surface ion density becomes lower. When the two charge collectors are connected through the external resistor, the output voltage decreases instantaneously to zero and no output electric energy can be detected by the current experimental setup, suggesting that due to the small surface areas of the Pt sheets, the harvested and stored LGH energy is trivial.

As the ion concentration (C) increases, $\mathrm{d}V/\mathrm{d}T$ of the Pt sheet is reduced. At a large solid–liquid interface, anions

are adsorbed on the electrode surface and forms the inner Helmholtz plane (IHP) [11]. The electrode potential can be described as [12]: $\phi = (\phi_e - \phi_{IHP}) + (\phi_{IHP} - \phi_b)$, where ϕ_e, ϕ_{IHP}, and ϕ_b are the potentials of the electrode surface, the IHP, and the bulk liquid phase, respectively. The potential drops can be expressed in terms of integral capacities (K); thus, $\phi = Q_e/K_e + Q_{IHP}/K_{IHP}$, where Q is the surface charge and the subscriptions of 'e' and 'IHP' indicate the electrode-IHP system and the IHP-bulk system, respectively. The overall interface capacitance is $C_i = dQ_e/d\phi$. Note that $Q_e = Q_{CA} + Q_{IHP}$, with Q_{CA} being the charge associated with the specifically adsorbed ions, and, consequently, $1 = dQ_{CA}/dQ_e + dQ_{IHP}/dQ_e$. Therefore, $1/C_i = 1/K_e - (1/K_{IHP})(dQ_{CA}/dQ_e)$. Since the IHP structure may be simplified as a monolayer, Q_{CA} is linear to the adsorption coverage (θ): $Q_{CA} = \alpha\theta$, with α being a system constant. Hence, $\phi = (1/K_e + 1/K_{IHP})\alpha\, d\theta$.

As a first-order approximation, the adsorption behaviors can be described by a Temkin isotherm [13]: $\theta = \ln \beta C/f = (k_B T/B) \ln[WC \exp(Q_o/k_B T)]$, where k_B is the Boltzmann constant, W is a parameter related to the molecular and ion distributions in the surface layer and in the bulk phase, B is a system constant related to the heat of adsorption, and Q_o is the heat of adsorption. Thus, $d\theta/dT = k_B \ln(WC)/B + (dQ_o/dT)/B$. We can then derive the equation for the temperature sensitivity: $|dV/dT| = -\{k_B A \ln(WC)/B + (dQ_o/dT)/B\}/K_{IHP}$. For the sake of simplification, it is assumed that the capacitance is independent of T, which is plausible for the discussion on ion concentration effects, since the change in C can be isothermal. Consequently,

$$\frac{1}{dC}\left|\frac{dV}{dT}\right| = -\frac{1}{K_{IHP}}\frac{k_B\alpha}{BC}. \quad (1)$$

Equation (1) explains why the output voltage (V) decreases as T rises, since all the parameters at the right-hand side (RHS) are positive. It also predicts that the temperature sensitivity of V ($|dV/dT|$) would be reduced as the ion concentration (C) becomes higher, which fits with the data of the reference experiments in figure 4.

However, compared with the reference system, the nanoporous carbon (NC) electrodes exhibit different characteristics of temperature dependence of electrode potential. First, as shown in figure 3, dV/dT is positive, suggesting that the electrode potential increases with temperature, which may be affected by the thermal behaviors of cations. Usually, on a neutral surface such as a platinum plate, anions are relatively easily adsorbed and form the IHP. Unlike the platinum plate, the NC under investigation is modified through acid treatment and surface oxidation. The NC surfaces have a large number of acidic functional groups, such as hydroxyl or carboxylic groups [14]. These negatively charged groups can suppress the adsorption of anions; therefore, the cations tend to promote the surface negativity. In addition, the adsorption parameters of cation, such as W, B and Q_o, are different from those of anion. Hence, the magnitude of $|dV/dT|$ should be different.

Second, as the ion concentration changes over a wide range from 0.1 to 3.7 M, there is not a clear pattern of the variation in $|dV/dT|$. When $C = 0.1$ M, the temperature sensitivity of the effective electrode potential is nearly 0.86 mV $°C^{-1}$; when $C = 1$ M, $|dV/dT|$ decreases to less than 0.75 mV $°C^{-1}$. While the trend looks similar with the prediction of the classic surface theory, when C further increases to 3.7 M, the temperature sensitivity rises back to 0.88 mV $°C^{-1}$. We may find the clue to explain this phenomenon in the analyses in [15, 16]. The negatively charged NC surface attracts positive ions and the co-ions also accompany to meet the local charge neutrality. In a nanopore of NC, this attraction can be intensified. The ion concentration in the nanopore should depend on the density of the surface groups, and is quite different from that in the bulk solution. We used the same NC for all the testing cells; therefore, the inner ion concentrations should not vary much. When we tested other monovalent salts, all the tests showed similar independence of the temperature sensitivity from the ion concentration. In addition, the high ion concentration in nanopores could result in a relatively low thermal sensitivity comparable to that of Pt plate in a highly concentrated solution.

4. Concluding remarks

It is clear that the above analysis is merely a qualitative, zero-order assessment of the thermal dependence of confined ion behaviors. It does not facilitate a fully developed model. Nevertheless, the experimental data validate that the thermally induced capacitive effect can be employed for LGH harvesting and storage. The thermal sensitivity of electrode potential can be much larger than the Seebeck coefficients of thermoelectric materials. As this effect is amplified by the large specific surface area of nanoporous materials, the energy density of TCS can be quite high. As temperature rises, the electrode potential of the nanoporous carbon under investigation increases, and its thermal sensitivity does not decrease monotonously, which are contradictory to the predictions of conventional surface theory.

Acknowledgment

This work was supported by the National Science Foundation under Grant No. ECCS-1028010.

References

[1] Lhermet H, Condemine C, Plissonnier M, Salot R, Audebert P and Rosset M 2008 *IEEE J. Solid-State Circuits* **43** 246
[2] Bell L E 2008 *Science* **321** 1457–61
[3] Quoilin S, Van den Broek M, Declaye S, Dewallef P and Lemort V 2013 *Renew. Sustainable Energy Rev.* **22** 168–86
[4] Zalba B, Marin J M, Cabeza L F and Mehling H 2003 *Appl. Therm. Eng.* **23** 251–83
[5] Velraj R, Seeniraj R V, Hafner B, Faber C and Schwarzer K 1999 *Sol. Energy* **65** 171–80
[6] Hung T C, Shai T Y and Wang S K 1997 *Energy* **22** 661–7
[7] Zhou S, Li X, Wang Z, Guo H and Peng W 2007 *Trans. Nonferr. Met. Soc. China* **17** 1328–33

[8] Nolas G S, Sharp J and Goldsmid J 2010 *Thermoelectrics: Basic Principles and New Materials Development* (Berlin: Springer)
[9] Liu L, Lim H, Lu W, Qiao Y and Chen X 2013 *Appl. Phys. Express* **6** 015202
[10] Lim H, Lu W and Qiao Y 2012 *Appl. Phys. Lett.* **101** 063902
[11] Bockris J O'M, Reddy A K N and Gamboa-Aldeco M 2000 *Modern Electrochemistry* 2nd edn, vol 2A (New York: Kluwer Academic) chapter 6, p 919
[12] Bockris J O'M, Reddy A K N and Gamboa-Aldeco M 2000 *Modern Electrochemistry* 2nd edn, vol 2A (New York: Kluwer Academic) chapter 6, p 960
[13] Frumkin A and Slygin A 1935 *Acta Physicochimica. URSS* **3** 791
[14] Huang Y 1972 *J. Catal.* **25** 131–8
[15] Cervera J, Schiedt B and Ramirez P 2005 *Eur. Lett.* **71** 35–41
[16] Siwy Z, Powell M R, Petrov A, Kalman E, Trautmann C and Eisenberg R S 2006 *Nano Lett.* **6** 1729–34